



Ecohydraulics of Surrogate Salt Marshes for Coastal Protection: Wave–Vegetation Interaction and Related Hydrodynamics on Vegetated Foreshores at Sea Dikes

Kara Keimer¹; David Schürenkamp²; Fenia Miescke³; Viktoria Kosmalla⁴; Oliver Lojek⁵; and Nils Goseberg, M.ASCE⁶

Abstract: Vegetation on foreshores in close vicinity to sea dikes may prove beneficial as regulating ecosystem service in the context of coastal defense, dike safety, and flood protection by reducing loads on these defense structures. Predominantly, a decrease in wave heights and bottom shear stresses is hypothesized, which calls for an inclusion in design procedures of coastal defense structures. In contrast to heterogeneous and variable salt marsh vegetation, this study uses surrogate vegetation models for systematic hydraulic experiments in a wave flume, without modeling specific plant species a priori. Froude-scale experiments are performed in order to investigate the effect of salt marsh vegetation on the wave transformation processes on the foreshore and wave run-up at sea dikes. The effect of plant and wave properties on wave transmission, energy dissipation, and wave run-up at a 1:6 sloped smooth dike are presented and discussed, focusing on the wave–vegetation–structure interaction. Vegetated foreshores can contribute to wave attenuation, where an increasing relative vegetation height h_v/h results in decreased wave run-up on the dike by up to 16.5% at $h_v/h = 1.0$. DOI: 10.1061/(ASCE)WW.1943-5460.0000667. This work is made available under the terms of the Creative Commons Attribution 4.0 International license, <https://creativecommons.org/licenses/by/4.0/>.

Introduction

The interaction and synthesis of ecology (vegetated foreshores) and hydraulics (wave action) has recently been termed “ecohydraulics”, and this field concerns fluid mechanics and engineering methods helping to foster a more thorough understanding of the complex plant–flow interactions (Carus et al. 2016; Maddock et al. 2013; Nestler et al. 2008; Spencer et al. 2016). Dunes, coastal forests, and salt marshes are examples for ecosystems that provide ecosystem services (ESS) relevant in conjunction with coastal defense and flood protection (Hanley et al. 2014; Kathiresan and Rajendran 2005; Silva et al. 2016). These have been classified as “natural” or “nature-based solutions” (Meselhe et al. 2020). In that context, the values and services provided by salt marshes are, e.g., blue carbon storage, habitat provision, ecosystem functioning, and the reduction of construction and maintenance cost, compared with dikes and sea walls without vegetated foreshores (King and Lester 1995; Barbier et al. 2011; Purcell et al. 2020).

Recent research on wave–vegetation interaction has revealed relevant percentages of wave attenuation due to wave energy

dissipation (King and Lester 1995; Koch et al. 2009) as well as reduction of currents and bed shear stresses and further, trapping, stabilization and covering of sediment by roots and rhizomes (Bouma et al. 2010; Cahoon et al. 1996). If a salt marsh erodes, it not only depends on the bed topography and the wave propagation, but also on sediment and vegetation characteristics forming the salt marsh bed (Christie et al. 2019).

It is hypothesized that salt marsh specific ESS can be related to the effects of foreshore geometry and characteristics of the salt marsh vegetation (Leonardi et al. 2018). Relevant hydrodynamic processes on the foreshore of sea dikes and within coastal salt marshes are (i) wave reflection at sea dikes and at the vegetation edges as well as (ii) wave energy dissipation within the salt marshes or rather wave transmission through vegetation on the foreshore to the toe of the sea dike. These processes along with (iii) wave–wave interactions reduce the wave heights impacting coastal defense structures such as sea dikes. Very often, decoupling of those interlaced processes remains very challenging, and counteracts the overall objective to establish predictive powers in those complex situations.

¹Leichtweiß-Institute for Hydraulic Engineering and Water Resources; Division of Hydromechanics, Coastal and Ocean Engineering, Technische Universität Braunschweig, Beethovenstraße 51a, 38106 Braunschweig, Germany (corresponding author). ORCID: <https://orcid.org/0000-0001-6064-5773>. Email: k.keimer@tu-braunschweig.de

²Leichtweiß-Institute for Hydraulic Engineering and Water Resources; Division of Hydromechanics, Coastal and Ocean Engineering, Technische Universität Braunschweig, Beethovenstraße 51a, 38106 Braunschweig, Germany. Email: d.schuerenkamp@tu-braunschweig.de

³Leichtweiß-Institute for Hydraulic Engineering and Water Resources; Division of Hydromechanics, Coastal and Ocean Engineering, Technische Universität Braunschweig, Beethovenstraße 51a, 38106 Braunschweig, Germany. Email: f.miescke@tu-braunschweig.de

Note. This manuscript was submitted on January 30, 2021; approved on June 4, 2021; published online on August 13, 2021. Discussion period open until January 13, 2022; separate discussions must be submitted for individual papers. This paper is part of the *Journal of Waterway, Port, Coastal, and Ocean Engineering*, © ASCE, ISSN 0733-950X.

⁴Leichtweiß-Institute for Hydraulic Engineering and Water Resources; Division of Hydromechanics, Coastal and Ocean Engineering, Technische Universität Braunschweig, Beethovenstraße 51a, 38106 Braunschweig, Germany. Email: v.kosmalla@tu-braunschweig.de

⁵Leichtweiß-Institute for Hydraulic Engineering and Water Resources; Division of Hydromechanics, Coastal and Ocean Engineering, Technische Universität Braunschweig, Beethovenstraße 51a, 38106 Braunschweig, Germany. ORCID: <https://orcid.org/0000-0003-1135-0105>. Email: o.lojek@tu-braunschweig.de

⁶Coastal and Ocean Engineering; Leichtweiß-Institute for Hydraulic Engineering and Water Resources; Division of Hydromechanics, Coastal and Ocean Engineering, Technische Universität Braunschweig, Beethovenstraße 51a, 38106 Braunschweig, Germany; Coastal Research Center; Joint Central Institution of the Leibniz Universität Hannover and the Technische Universität Braunschweig, Merkurstraße 14, 30419 Hannover, Germany. ORCID: <https://orcid.org/0000-0002-1550-3001>. Email: n.goseberg@tu-braunschweig.de

Previous Results on Wave Attenuation

Numerous researchers have put great efforts into the quantification of wave height and wave energy reduction through coastal salt marshes. Wave energy dissipation is not only dependent on various vegetation and wave parameters, but also on the complex interaction of those parameters that vary in space and time (Koch et al. 2009), thus making it difficult to provide a simple equation to quantify the wave height reduction due to a foreshore geometry and a coastal salt marsh. Consequently, for this study it is important to determine the most influential parameters governing wave run-up reduction at coastal sea dikes. Augustin et al. (2009) observed that wave energy dissipation increases with decreasing water level, Anderson and Smith (2014) and Peruzzo et al. (2018) point out an increased wave energy dissipation with increasing vegetation density, whereas Rupprecht et al. (2015) reported that wave reduction is more dependent on vegetation biomass and plant stiffness. All in all, previous investigations emphasized a general correlation between vegetation characteristics and the reduction of wave parameters, however these effects have not been quantified comprehensively because the processes are not yet deciphered fully.

More specifically, the extent of wave energy dissipation through meadows also depends on vegetation parameters such as plant height, diameter, stiffness, density, and the spatial arrangement or rather biomass along with their ecological niche-dependent zonation along the foreshore (John et al. 2015; Schoutens et al. 2020; Tempest et al. 2015). The properties of salt marsh vegetation growing in the vicinity of the marsh edge towards the ocean are found to respond through avoidance with respect to the wave-induced stresses, as compared with those growing further onshore. Thus, plants growing in different salt marsh zonation are considered to influence wave damping according to their site-specific properties (Schoutens et al. 2020). The wave energy dissipation also depends on wave parameters such as wave height and period as well as water depth and (wave-induced) currents (John et al. 2015; Vuik et al. 2016; Paul et al. 2012; Tempest et al. 2015). Leonardi and Fagherazzi (2015) stated that the effect on salt marshes due to extreme storm surge events depends on the general exposure of the salt marsh to heavy, storm-induced, wave events. It was shown that salt marshes exposed to higher wave loads more frequently exhibited less damage in extreme wave conditions, whereas salt marshes exposed to less strong wave conditions on average sustained a higher level of damage during extreme events.

Wave Analysis Methods

To generally distinguish between incoming and reflected wave energy, a set of methods can be applied (Goda and Suzuki 1977; Mansard and Funke 1980; Hughes 1993). However, owing to effects in shallow water, with mildly sloped bottom elevation, and wave breaking close to structures or obstacles (coastal salt marsh) it remains unclear to date how accurate these methods are. These processes are likely exacerbated by the effects salt marshes have on wave and current propagation, because they reduce the water depth while also inducing turbulence. McCowan (1891) gives a ratio of wave height H to water depth h below $H/h < 0.78$ where wave breaking is stipulated; a threshold most often reached and, thus, wave breaking is a common feature in shallow, submerged coastal salt marshes during storm surge events. As a result of wave breaking, energy dissipation and wave height reduction will occur.

Along with the above-mentioned processes reflection and transmission, it is also important to consider wave set-up at sea dikes and a possible effect on wave set-up development due to the presence of a vegetated foreshore. Wave set-up and set-down occur due

to wave shoaling, breaking and run-up at sea dikes, where the wave set-up can be basically described as a function of the bathymetry and dike slope, water depth, wave height, and wave period (EurOtop 2018; Stockdon et al. 2006; Liebisch 2015). With a coastal salt marsh located seaward of the dike profile, those parameters will be influenced which likely results in a change of wave set-up. As static wave set-up results from a transfer of wave energy to the water column due to wave breaking and energy dissipation, it is assumed that this energy transfer will also be reduced through increased bottom friction over vegetated foreshores (Dean and Bender 2006).

Nonetheless, the most important parameters determining the crest height of coastal dikes remain the wave run-up and the acceptable wave overtopping discharge q_{adm} , e.g., after EurOtop (2018). To predict wave run-up on coastal sea dikes, EurOtop (2018) provides a set of equations derived from a plethora of experimental investigations and related studies largely based in Europe, although the manual is still suitable for worldwide application. It gives guidance in regards to overtopping calculations and management at coastal protection structures. The manual states that the relative wave run-up often sought as a prime parameter for dike design depends on the wave height at the toe of the structure, the surf similarity parameter, and the configuration of foreshore and dike. Wave height decreases due to wave breaking resulting from decreased water depth and increased wave steepness on the foreshore. In order to estimate the average wave run-up and overtopping on sea dikes, it is of paramount importance to use the appropriate wave parameters. Experimental investigations of van Gent (2001) show that the use of the shallow-water peak period T_p may lead to disproportionate high values of the surf-similarity parameter due to higher energy transfer to lower wave frequencies in shallow water. However, the use of the peak period T_p in deep water may cause underestimation in the prediction of wave run-up (van Gent 2001). It is more advantageous to use the spectral wave period $T_{m-1,0}$, which gives more weight to the longer wave periods in a spectrum (EurOtop 2018; van Gent 2001). Furthermore, to include the effect of wave transformation on the incident wave running up the sea dike, the spectral wave height at the toe of the structure should be used (EurOtop 2018).

Objectives of This Study

In the past, a number of laboratory investigations have been carried out to examine the ecohydraulic implications of salt marsh vegetation, with both live and idealized surrogate vegetation (Anderson et al. 2013; Anderson and Smith 2014; Augustin et al. 2009; Maza et al. 2015; Möller et al. 2014; Tschirky et al. 2001). In addition, some investigations were dedicated to the wave-vegetation interaction without focusing on salt marshes (Hu et al. 2014; Koftis et al. 2013; Mei et al. 2011). Currently, however, the effect of complex foreshore processes on key design parameters such as wave run-up and overtopping dynamics influenced by vegetation have not yet received sufficient attention.

Several knowledge gaps that concern the interaction of vegetated foreshores and wave action can be identified, i.e., (i) determining the interaction between ecohydraulic processes on foreshores and coastal structures, (ii) quantifying the effect of different meadow heights, geometries, densities, rigidities, and arrangements as well as (iii) developing equations and design guidelines for coastal structures such as sea dikes including vegetated foreshores. These knowledge gaps are most prevalent in the context of wave loading on sea dikes. The reduction of wave run-up and overtopping are the main concerns for safety and stability of sea dikes from a coastal protection perspective, because crest heights of structures are designed with an acceptable wave overtopping discharge defined. In case of shallow

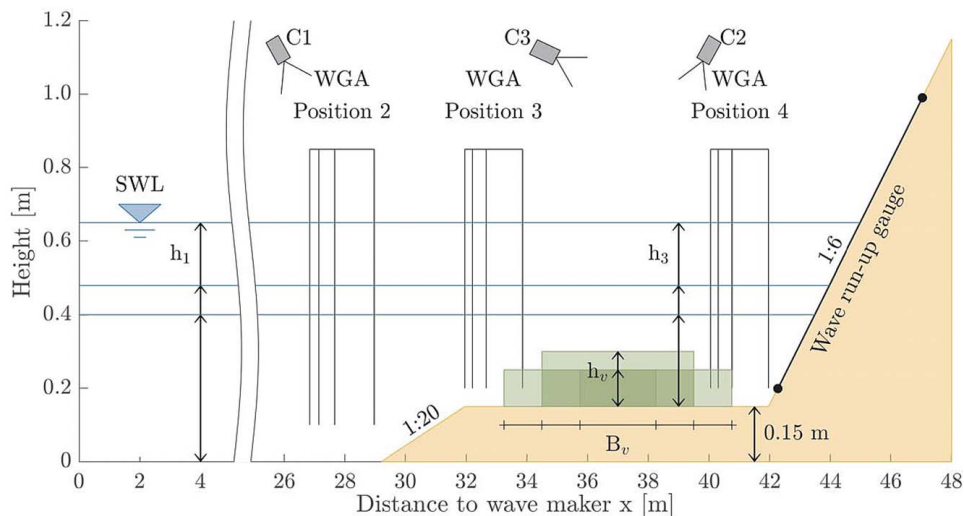


Fig. 1. Model setup in the wave flume (width 1.0 m) with vegetation field on the foreshore and 1:6 sloped dike, as well as positions of the instrumentation. (WGA = wave gauge arrays; SWL = still water level).

foreshores, the averaged overtopping discharge is often overestimated by common design equations. However, vegetated foreshores are not adequately considered to date (EurOtop 2018; Altomare et al. 2016), owing to insufficient experimental data and scientific understanding regarding vegetation related wave run-up and energy dissipation effects.

The overall objective of this study is to contribute to a better understanding of ecohydraulic processes by expanding state-of-the-art knowledge on wave energy dissipation and wave run-up by vegetated foreshores employing physical modeling. Based on this motivation and the identified knowledge gaps, the specific objectives of this study are to (i) investigate the reduction potential of surrogate vegetation on wave loads (wave run-up height) at sea dikes with focus on vegetation density, submergence depth and meadow width; as well as the effects (ii) on wave reflection, wave transmission, and wave set-up at sea dikes and (iii) the identification of processes and relevant dimensionless parameters, other than the drag coefficient of vegetated foreshores, which should be considered in sea dike assessment.

The remainder of this work is organized as follows. The section “Methodology and study design basis” contains the basis of the design of this study as well as test setup and experimental program. The section on “Results” consists of analysis pertaining to wave reflection, transmission, and wave height reduction within the vegetation model on the foreshore, as well as reductions of the wave set-up and run-up on the sea dike structure. The “Discussion” section sets the obtained results in perspective before final conclusions are drawn in the “Conclusions” section.

Methodology and Study Design Basis

Based on the above-outlined knowledge gaps, and urgent need for a better understanding of the feedback interaction between salt marsh vegetation and wave hydrodynamics, the effect on the wave run-up of vegetated foreshores situated in front of coastal dikes is the focal point of this work. Based on theoretical and experimental investigations, the ecohydraulic processes wave breaking, wave attenuation, and wave energy dissipation are analyzed. These often occur where waves interact with vegetated foreshores. A comprehensive set of physical experiments is performed in a wave flume (see Fig. 1), where surrogate foreshore vegetation is used. Mildly

flexible stem specimen approximated individual plants. A more thorough scaling of plants by the application of Cauchy similitude (e.g., bending modulus E , second moment of stem cross-sectional area I) remains a task for future study. The experiments focus on the overall effect of coastal salt marshes and, thus, the characteristics of specific plant species are not modeled individually. Stem diameters were not scaled individually by Froude similitude, but the meadows were considered as arrangements of staggered stems with a relative stiffness. This approach was chosen in order to overcome scaling problems related to density, buoyancy, and elastic forces as discussed among others in Anderson and Smith (2014) and Wu and Cox (2015). Different meadow configurations regarding width, plant density, and stem height were investigated for their hydrodynamic effects compared against a nonvegetated base. This study uses a wide range of the submergence depth of the foreshore vegetation, defined as a ratio of water level h to vegetation height h_v . The novel investigation of wave attenuation and its overall effect on wave run-up on a dike is studied in the range of $h_v/h = 0.2$ up to 1.0. To enhance the comparability, dimensionless parameters are used to analyze and comprehend the transformation processes for this study. To consider the influence of the foreshore geometry for the analysis, the laboratory tests with vegetation are compared with the equivalent test without vegetation (coated plywood model) as a reference.

An analysis of the foreshore geometries at the coastline of Lower Saxony, Germany (320.1 km; excluding estuaries) with 177.7 km sea dike line including foreshore was analyzed along cross sections every 100 m. The front slope of the foreshore until it reaches the mean high tide was neglected. The results for the mean foreshore slopes (after smoothing the profiles to neglect trenches) show 82% to be greater or smaller than $\pm 0.2\%$ (62% greater or smaller than $\pm 0.1\%$), where positive values indicate an upward slope towards the sea dike and vice versa. This reveals that most foreshores are fairly plain and just slightly sloped. Thus, the foreshore can be approximated as a horizontal profile in most cases.

Six different experimental configurations with surrogate models of foreshore vegetation and a series of reference conditions without vegetation have been tested in a wave flume. The wave flume was equipped with a piston-type wave maker (manufacturer: HR Wallingford), located at the Leichtweiß-Institute for Hydraulic Engineering and Water Resources (LWI, Technische Universität Braunschweig, Germany). The test setup and the experimental program are described next.

Table 1. Absolute distance between the wave maker and each wave gauge of a wave gauge array

Wave gauge (-)	WGA _{pos2} (m)	WGA _{pos3} (m)	WGA _{pos4} (m)
1	26.84	31.96	40.06
2	27.14	32.21	40.31
3	27.66	32.66	40.76
4	28.96	33.86	41.96

Test Setup

An experimental setup representing a foreshore–dike combination with and without vegetation specimen is used in the wave flume, modeled at medium scale of 1:10 with an overall length of 90 m, horizontal bottom, and a width of 1.0 m. The scaled model, designed in accordance with German foreshore conditions as presented in the previous section, consists of a transition slope ($\tan \alpha_2 = 1 : 20$) starting at a distance of 29.0 m from the piston-type wave maker in front of a horizontal foreshore profile ($\tan \alpha_3 = 0$) with the width of 10.0 m and a dike profile ($\tan \alpha_4 = 1 : 6$) with a total height of the dike model $h_D = 1.0$ m as shown in Fig. 1. Cameras were installed to have visual support to document the wave transformation processes. The first camera (C1) was filming the transition slope, the second camera (C2) the meadow, and the third camera (C3) was used to observe the wave run-up on the dike. All three camera models were Panasonic HC-V250 with 10 MP resolution and 50 fps. The experimental setup (transition slope, foreshore, and dike) was constructed using aluminum profiles as a subconstruction on which smooth marine grade plywood boards were mounted. The first 40 cm length of the transition slope in front of the foreshore was build using fine concrete to begin the 1:20 slope. Any transitional sections of the construction were smoothed out with silicone and the gap between the dike profile and the walls was sealed for accurate run-up measurements.

The wave flume has been instrumented with three custom-made and calibrated wave gauge arrays (each with four wave gauges with a sample rate of 60 Hz) in front of the transition slope (WGA_{pos2}), on the foreshore in front of the vegetation (WGA_{pos3}), and at the toe of the dike (WGA_{pos4}). Table 1 lists the distance of each wave gauge within a wave gauge array to the wave maker.

The characteristics of incident and reflected waves were analyzed for all tests according to the reflection analysis method by Mansard and Funke (1980) and compared with the reference tests. Wave run-up gauges (also custom made and calibrated) on the dike with a range of the run-up height between 4.5 and 84.0 cm (42.27 to 47.04 m from the wave maker) and a sample rate of 60 Hz were calibrated and used for the analysis of wave run-up and wave set-up. The gauges were positioned in the center of the flume to reduce the effect of the side walls. The gauges consist of equally spaced measuring pins, with a distance of 1.0 cm which triggers a signal when contacted by water. The wave run-up has been validated by a video analysis (C3) with markings on the dike each 5.0 cm, which are shown in Fig. 2.

Experimental Program

The following range of wave parameters of regular waves were tested (all parameters in model scale) without targeting and representing specific wave properties, but in a range of natural wave conditions: wave height $H_{m0,1} = 0.08$ – 0.20 m and peak period $T_{p,1} = 1.0$ – 5.0 s. These were chosen to systematically investigate a wide range of wave properties. The waves were generated in a water depth at the wave maker of $h_1 = 0.42$ – 0.67 m and on the foreshore $h_3 = 0.25$ – 0.50 m, respectively. These water depths were

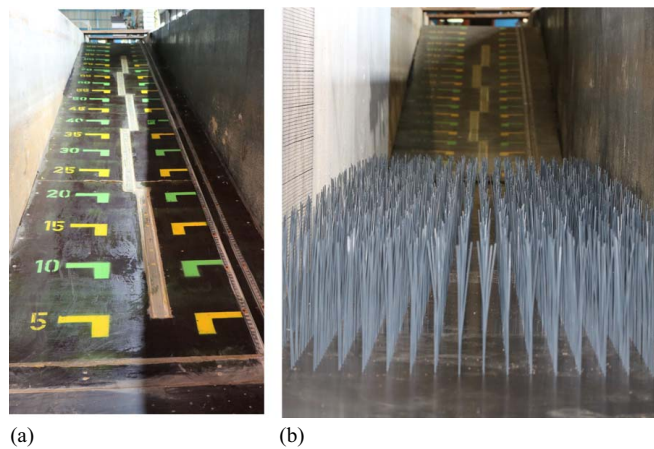


Fig. 2. Pictures of the experimental setup in the 1 m wide flume: (a) view at the dike; and (b) view at artificial vegetation ($n_v = 400 \text{ m}^{-2}$, $h_v = 0.25$ m, and $B_v = 5.0$ m).

selected for a systematic investigation as well, not in regards to conditions found in nature. Low and high coverings of vegetation were chosen to consider storm flood conditions, which are most relevant in the design of coastal protection structures. Even though regular waves were generated, the analysis is conducted using spectral wave parameters (H_{m0} and $T_{m-1,0}$) instead of time domain parameters to include the effect of wave transformations and reflection, because shallow and intermediate conditions caused nonlinear (irregular) waves to form and propagate to the foreshore geometry.

Two vegetation heights were investigated: $h_v = 0.10$ and $h_v = 0.25$ m. As a result, relative vegetation heights, defined as vegetation height h_v over the local water depth h_3 (on the horizontal foreshore), were investigated in a range of $h_v/h_3 = 0.20$ – 1.00 . To include variations in water depth, the actual still water depth on the foreshore was determined using the wave run-up gauge measurements before wave generation. The mean difference between target and actual water depth was 1.9 ± 0.5 cm. Owing to the small difference, the results will be summarized for the relative vegetation height h_v/h_3 using the theoretical water depth. The following nondimensional parameters at the front of the foreshore profile at position 2 ($x_{\text{WGApos2}} = 27.9$ m) were determined and used as incoming wave parameters:

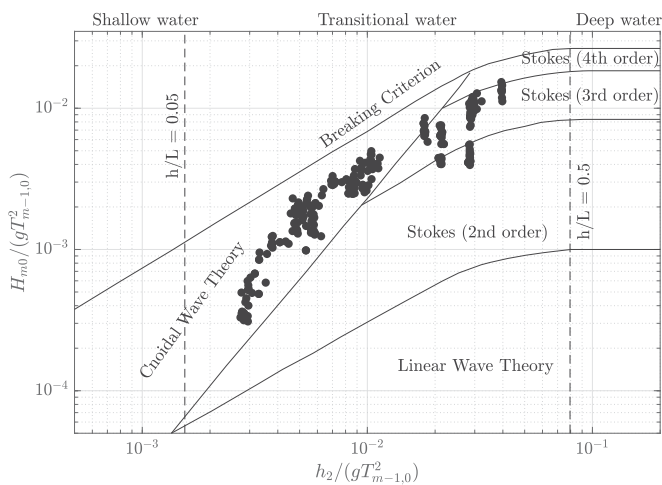
- relative vegetation width (vegetation width B_v over wave length $L_{m-1,0}$ in front of the foreshore), $B_v/L_{m-1,0} = 0.21$ – 5.24 ;
- wave steepness (wave height H_{m0} over wave length $L_{m-1,0}$), $H_{m0}/L_{m-1,0} = 0.01$ – 0.10 ;
- the relative water depth (local water depth h_2 in front of the foreshore over wave length $L_{m-1,0}$), $h_2/L_{m-1,0} = 0.05$ – 0.27 (transitional waves);
- and the surf similarity parameter, $\xi_{m-1,0} = 0.54$ – 3.78 .

The incoming wave parameters were considered (at position 2), because they differ from the nominal wave properties of the wave maker owing to wave transformations and wave–wave interactions between the wave maker and the model boundary.

The surf similarity parameter was calculated using the dike slope of 1:6 and the deep-water wave length $L_{0,m-1,0}$, which was determined from the wave period $T_{m-1,0}$ at position of WGA_{pos2} (EurOtop 2018). Wave reflection compensation at the wave maker was active. A summary of the tested hydraulic conditions is given in Table 2 for position 2 in front of the foreshore model. This test program was carried out for each configuration and the difference in incoming wave properties for the tests of different

Table 2. Hydraulic parameters of the test program (*r*-regular, *j*-JONSWAP)

No. (-)	Nominal				waves (-)	Measured at position 2 in front of the foreshore					
	$H_{m0,1}$ (m)	$T_{p,1}$ (s)	h_2 (m)			H_{m0} (m)	$T_{m-1,0}$ (s)	$L_{m-1,0}$ (m)	$h_2/L_{m-1,0}$ (-)	$H_{m0}/L_{m-1,0}$ (-)	H_{m0}/h_2 (-)
1	0.08	5.0	0.385 ± 0.002		<i>r</i>	0.111 ± 0.010	3.264 ± 0.115	6.268	0.062	0.018	0.287
2	0.12	1.0	0.387 ± 0.001		<i>r</i>	0.131 ± 0.012	0.998 ± 0.001	1.433	0.270	0.092	0.339
3	0.12	1.5	0.386 ± 0.002		<i>r</i>	0.150 ± 0.016	1.480 ± 0.006	2.560	0.151	0.059	0.390
4	0.12	2.0	0.386 ± 0.001		<i>r</i>	0.161 ± 0.014	1.949 ± 0.009	3.592	0.108	0.045	0.418
5	0.12	3.0	0.385 ± 0.002		<i>r</i>	0.158 ± 0.010	2.325 ± 0.089	4.373	0.088	0.036	0.411
6	0.12	4.0	0.386 ± 0.001		<i>r</i>	0.141 ± 0.010	2.677 ± 0.114	5.097	0.076	0.028	0.366
7	0.12	5.0	0.386 ± 0.002		<i>r</i>	0.163 ± 0.009	2.817 ± 0.073	5.378	0.072	0.030	0.423
8	0.08	1.5	0.461 ± 0.004		<i>r</i>	0.092 ± 0.004	1.490 ± 0.002	2.741	0.168	0.034	0.201
9	0.08	3.0	0.458 ± 0.009		<i>r</i>	0.104 ± 0.013	2.859 ± 0.040	5.924	0.077	0.018	0.227
10	0.08	5.0	0.461 ± 0.002		<i>r</i>	0.085 ± 0.009	3.943 ± 0.119	8.311	0.056	0.010	0.185
11	0.12	1.5	0.461 ± 0.003		<i>r</i>	0.141 ± 0.015	1.483 ± 0.007	2.725	0.169	0.052	0.305
12	0.12	4.0	0.461 ± 0.004		<i>r</i>	0.156 ± 0.014	3.009 ± 0.115	6.269	0.074	0.025	0.340
13	0.08	1.5	0.626 ± 0.004		<i>r</i>	0.102 ± 0.011	1.497 ± 0.002	3.010	0.208	0.039	0.163
14	0.08	5.0	0.627 ± 0.002		<i>r</i>	0.077 ± 0.008	4.705 ± 0.137	11.571	0.054	0.007	0.127
15	0.16	1.5	0.627 ± 0.002		<i>r/j</i>	0.201 ± 0.023	1.492 ± 0.005	2.996	0.209	0.067	0.321
16	0.16	3.0	0.627 ± 0.001		<i>r/j</i>	0.192 ± 0.021	2.670 ± 0.100	6.330	0.099	0.030	0.307
17	0.16	5.0	0.627 ± 0.001		<i>r/j</i>	0.179 ± 0.015	3.576 ± 0.163	8.703	0.072	0.021	0.285
18	0.20	1.5	0.627 ± 0.003		<i>r</i>	0.232 ± 0.021	1.464 ± 0.018	2.910	0.215	0.080	0.370
19	0.20	3.0	0.627 ± 0.002		<i>r</i>	0.239 ± 0.025	2.553 ± 0.107	6.017	0.104	0.040	0.380

**Fig. 3.** Incoming wave parameters (H_{m0} , $T_{m-1,0}$) at position 2 shown for the wave theory classification after CERC (1984).

configurations is shown by the mean value joined with standard deviation.

The wave-theoretical classification of the waves used in this study is provided in Fig. 3, based on the incoming spectral parameters H_{m0} and $T_{m-1,0}$ at position 2 after CERC (1984). Most of the tests used regular waves, however, some of the tests (as per Table 2) were carried out with a JONSWAP-spectrum for the configurations 0, 5 and 6 (Table 3). For the test numbers 14 and 16 without vegetation (configuration 0), the wave run-up observed at the dike profile was higher than the wave run-up gauges (video validation).

The six tested meadow configurations are listed in Table 3. Reference tests without vegetation were performed for each tested hydraulic condition (configuration 0). These reference tests are used for the comparison of wave set-up η_s and wave run-up $R_{it2\%}$ with and without foreshore vegetation. To improve the identification of outliers due to the variance of incoming wave parameters and, therefore, wave transformation, most tests (including the reference tests) were carried out twice.

Uniformly arranged idealized vegetation models were used to simulate a generic vegetation field on the foreshore consisting

Table 3. Tested configurations with surrogate vegetation

Configuration (-)	Meadow width B_v (m)	Meadow height h_v (m)	Meadow density n_v (m ⁻²)
0 (reference)	0.0	0.00	0
1	5.0	0.25	400
2	5.0	0.25	200
3	5.0	0.10	200
4	5.0	0.10	400
5	7.5	0.10	400
6	2.5	0.10	400

of cylindrical polyvinyl chloride (PVC) rods with a diameter of $d_v = 3$ mm and a bending stiffness of $EI = 13.121$ N mm². In the context of the coastal protection and the dike safety, the vegetation model was designed for a low shoot density compared with field measurements (see, for example, Abu Hena et al. 2007) and narrow vegetation fields (25–75 m considering the 1:10 scale). Considering the foreshore width of 10 m, the ratio of meadow width to foreshore width ranges from 0.25 to 0.75. In comparison, unpublished preliminary analysis of the Lower Saxony coastline, Germany, shows 40% of the foreshore widths are up to 300 m, where only widths over 50 m were accounted for due to the idealized calculation of foreshore width.

The characteristics of the vegetation model, such as elastic forces and the dynamic behavior under wave action were not designed for a specific plant species specifically. The investigated variation of local water depths h_3 and vegetation heights h_v are shown in Fig. 4. Since the influence of the foreshore geometry on the wave characteristics increases with decreasing water depth, the wave transformation processes need to be investigated separately for each water depth for an overall understanding. Hence, the results in this study are shown for each water depth separately and compared for both vegetation heights.

Data Analysis

The three wave gauge arrays (see Fig. 1) were analyzed to determine the local wave heights over the test duration of 10 min, including around 5–10 s measurement before starting the wave generation to determine the still water level. The waves generated by the

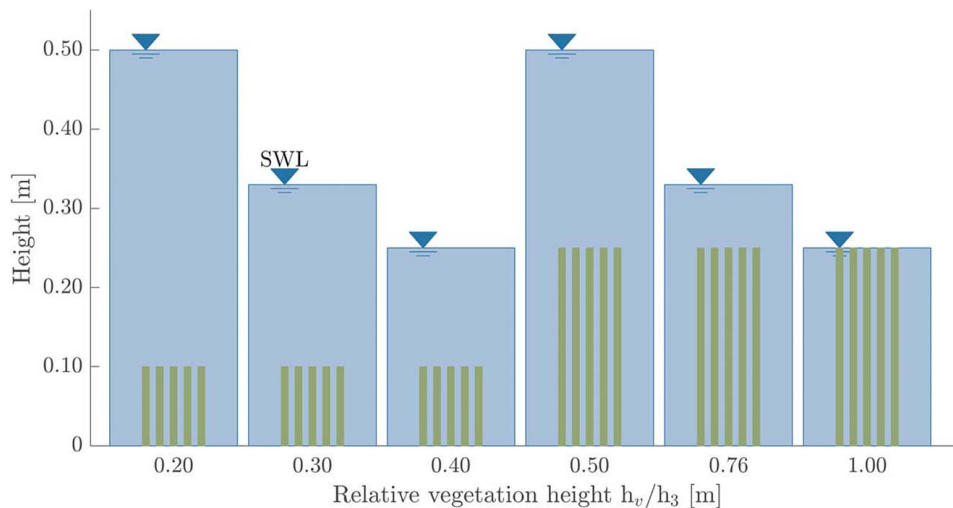


Fig. 4. Tested combinations of vegetation height h_v and local water depth h_3 with relative vegetation height h_v/h_3 .

ramping up are neglected in the reflection analysis as well as for the wave run-up gauges. The incident and reflected wave parameters (zeroth moment of the wave spectrum m_0 , wave height H_{m0} , and wave period $T_{m-1,0}$) are determined by reflection analysis according to Mansard and Funke (1980). As the peaks of the generated wave spectra are shifted in shallow water by spectral transformation (Mahmoudof et al. 2016; Ardani and Kaihatu 2019), the wave heights and periods were analyzed applying the fast Fourier transform (FFT) technique and the following equations:

$$H_{m0} = 4 \cdot \sqrt{m_0} = 4 \cdot \sqrt{\sum_{i=1}^n S(f)_i \Delta f} \quad (1)$$

$$T_{m-1,0} = m_{-1}/m_0 \quad (2)$$

where $S(f)$ is the spectral density, n is the number of frequency components, and Δf the frequency resolution. A high-pass filter ($f_p/2.1$ Hz) as well as a low-pass filter ($f_p \cdot 3.1$ Hz) were applied to cutoff the spectrum with the nominal peak wave frequency ($f_p = 1/T_p$). Comparing the wave heights $H_{1/3}$ (determined using zero down-crossing) and the zeroth-moment wave heights H_{m0} , it was found that H_{m0} is, on average, about 26.6% higher than $H_{1/3}$. It is hypothesized that small dissipated wave components are overlooked by the zero down-crossing method. For the analysis, the spectral wave parameters (H_{m0} and $T_{m-1,0}$) will be used because shifting wave spectra were observed, whereas the spectra themselves and changes due to foreshore geometry and surrogate vegetation are not analyzed as part of this study.

In addition, the effects of the wave generation and the flume bottom/walls were taken into account for the investigations by the analysis of the incident wave parameters at position 2 (WGA_{pos2}) in front of the foreshore profile. As shown in Table 2, waves were generated with varying wave heights and wave periods to investigate the influence of the incoming wave characteristics. For the long waves with a generated peak period of $T_{p,1} = 5$ s, wave dispersion processes causing a transformation of the wave spectrum especially for low water depths at the wave maker where orbital velocities were immediately being felt by the flume bottom during shallow and intermediate conditions. To consider this effect, the wave gauge array at the foreshore toe was analyzed and considered for the comparison of wave transmission and wave run-up by using the incoming wave properties in front of the foreshore instead of generated wave parameters. The incoming wave properties were

analyzed based on the method of Mansard and Funke (1980) on a horizontal bed with four wave gauges. As only three wave gauges are needed, four different wave gauge combinations could be used to determine the best match for the requirements after Mansard and Funke (1980) in consideration of the large experimental program and the varying wave lengths due to a wide range of wave properties.

The first analyzed process is wave reflection, which is shown as the reflection coefficient $K_{r(2)}$ and was determined as the ratio of the reflected and incident zeroth moments of the wave energy with the following equation:

$$K_{r(2)} = \sqrt{m_{0,i}}/\sqrt{m_{0,r}} = H_{m0,i}/H_{m0,r} \quad (3)$$

where $K_{r(2)}$ is the wave reflection coefficient, $m_{0,i}$ is the zeroth moment of the incident wave energy spectrum, $m_{0,r}$ is the reflected wave energy spectrum, $H_{m0,i}$ is the incident wave height, and $H_{m0,r}$ is the reflected wave height.

The second process is wave attenuation, which is expressed through the transmission of the wave energy across the vegetation field by employing the wave transmission coefficient $K_{t(4,2)}$, with the zeroth moment of the wave energy at position 2 (in front of the foreshore profile and vegetation field) and position 4 (behind the vegetation field) as follows:

$$K_{t(4,2)} = \sqrt{m_{0,4}}/\sqrt{m_{0,2}} = H_{m0,4}/H_{m0,2} \quad (4)$$

where $K_{t(4,2)}$ is the transmission coefficient based on the zeroth moment m_0 , or the incoming spectral wave height H_{m0} at the positions 2 and 4.

In addition to the wave transformation on the foreshore, wave set-up η_s in front of the dike was investigated, because a higher wave set-up owing to obstructed return flow often generates a higher wave run-up. The wave run-up gauges (see Figs. 1 and 2) were used to determine the wave set-up (Liebisch 2015; Dean and Walton 2010). The time frame for calculating the wave set-up starts as soon as the wave run-up gauges measure a value above still water level, which was determined by the first measured values before wave generation, and ends after 10 min test time are over. A mean water level for the wave run-up gauges was determined during the tests. The difference between the mean water level during waves running up the dike profile and the still water level was set as the wave set-up, which can be summarized as a change in mean water level in front of the sea dike. To evaluate the change of wave set-up $\Delta_{\text{set-up}}$ owing to the foreshore vegetation,

tests with and without vegetation were compared, by evaluating

$$\Delta_{\text{set-up}} = (1 - \eta_{s,\text{veg}}/\eta_{s,\text{ref}}) \cdot 100\% \quad (5)$$

where $\eta_{s,\text{veg}}$ is the wave set-up with vegetation and $\eta_{s,\text{ref}}$ is the wave set-up in the reference case without vegetation.

The results of this study for wave set-up were compared with the equation presented by Liebisch (2015), which reads as follows:

$$\eta_s/L_0 = 0.061 \cdot 0.402^{\xi_m} \quad (6)$$

where the relative wave set-up η_s/L_0 is calculated using the surf similarity parameter ξ_m regarding the mean wave height and period.

The fourth process analyzed in this study is the wave run-up $R_{u2\%}$, which is measured with wave run-up gauges on the dike. For each wave, the maximum vertical run-up height was identified. The reduction of the wave run-up due to foreshore vegetation is determined as the relation of the different vegetation configurations to the corresponding reference test, evaluating the following equation:

$$\Delta_{\text{run-up}} = (1 - R_{u2\%(\text{veg})}/R_{u2\%(\text{ref})}) \cdot 100\% \quad (7)$$

where $R_{u2\%(\text{veg})}$ is the 2% exceeding wave run-up height with foreshore vegetation and $R_{u2\%(\text{ref})}$ is the wave run-up height of the reference case without vegetation.

To determine a relation, a comparison with equations by EurOtop (2018) is implemented in this study. The equations after EurOtop (2018) are

$$R_{u2\%}/H_{m0} = 1.65 \cdot \gamma_b \cdot \gamma_f \cdot \gamma_\theta \cdot \xi_{m-1,0} \quad (8)$$

with a maximum of

$$R_{u2\%}/H_{m0} = 1.00 \cdot \gamma_f \cdot \gamma_\theta \cdot \left(4 - 1.5/\sqrt{\gamma_b \cdot \xi_{m-1,0}}\right) \quad (9)$$

The influence factor for the berm $\gamma_b=1.0$, the roughness $\gamma_f=1.0$, and the wave attack angle $\gamma_\theta=1.0$ are set to unity, in order to focus on the effects of the vegetation within the framework of the EurOtop (2018) method application. The breaker parameter is calculated using the dike slope, i.e., 1:6, as well as the wave steepness $H_{m0}/L_{m-1,0}$ with $L_{m-1,0}$ being the deep-water wave length determined with the local wave period $T_{m-1,0}$ at the toe of the dike (EurOtop 2018).

Results

The results of this study indicate the most significant influence for the relative vegetation height, which is why this is the parameter chosen for the analysis. The analyzed parameters could not be shown as a function of relative vegetation width or density because of a large scatter due to varying incoming wave properties. Still, the results for the different vegetation configurations are listed in tables and tendencies are evident in some cases.

The results are shown using boxes for the wide range of wave properties, which were generated in this study. The line in the box-plot graphs indicates the median value and the box limits show the 25% and 75% quartile (interquartile range). The markers show outliers, which are defined to be higher or lower than 1.5 times the interquartile range. Tables are used to present the influence of the meadow configurations, summarizing different wave properties as well as water depths.

Wave Reflection

The reflection coefficients were analyzed at the wave gauge array in front of the foreshore profile (WGA_{pos2}) and in front of the meadow

Table 4. Reflection coefficients K_r of different vegetation configurations (at positions 2 and 3)

Configuration (-)	Surrogate meadow			Reflection coefficient	
	B_v (m)	h_v (m)	n_v (m ⁻²)	$K_{r(2)}$ (-)	$K_{r(3)}$ (-)
0 (reference)	0.0	0.00	0	0.165 ± 0.090	0.190 ± 0.090
1	5.0	0.25	400	0.154 ± 0.088	0.177 ± 0.090
2	5.0	0.25	200	0.151 ± 0.086	0.185 ± 0.090
3	5.0	0.10	200	0.158 ± 0.091	0.187 ± 0.096
4	5.0	0.10	400	0.160 ± 0.099	0.188 ± 0.102
5	7.5	0.10	400	0.146 ± 0.079	0.173 ± 0.077
6	2.5	0.10	400	0.197 ± 0.129	0.189 ± 0.104

(WGA_{pos3}). The reflection coefficients for position 2 varied between 0.075 and 0.484 (with a mean value of 0.165 and a standard deviation of 0.090) for the reference case without vegetation and between 0.060 and 0.528 (with a mean value of 0.160 and a standard deviation of 0.095) for the vegetated experiments. At position 3, the reflection for the reference varied between 0.062 and 0.497 (with a mean value of 0.190 and a standard deviation of 0.090). For all vegetation configurations values between 0.058 and 0.490 (with a mean value of 0.183 and a standard deviation of 0.092) were found. Table 4 lists the resulting reflection coefficients for the wave gauge array WGA_{pos2} in front of the foreshore and WGA_{pos3} in front of the meadow depending on the configuration, which result from the meadow width (B_v), the meadow height (h_v), and the meadow density (n_v).

Comparing the results for different meadows (Table 4), no significant tendency is apparent for the wave reflection considering different vegetation densities (configurations 1 and 2 for $h_v=0.25$ m; configurations 3 and 4 for $h_v=0.10$ m) or vegetation heights (configurations 1 and 4 for 400 m⁻²; configurations 2 and 3 for 200 m⁻²). However, a higher reflection coefficient can be seen for position 3 in front of the meadow as compared with position 2 in front of the foreshore toe.

Fig. 5 shows the effect of the relative vegetation height on the wave reflection coefficient K_r for position 2 in front of the foreshore $K_{r(2)}$ and at position 3 in front of the vegetation on the foreshore $K_{r(3)}$. The results for all configurations are shown in Fig. 5.

Fig. 5 shows that reflection is mainly influenced by the foreshore geometry and not by the meadow. As the reflection is relatively low in general, the effect of the relative vegetation height cannot be identified clearly. The results show a similar behavior for position 2 and position 3. Although a higher reflection is apparent for $K_{r(3)}$ with the water depth $h_3=0.33$ m, a clear difference cannot be observed because the variance is not significant. At both positions an influence of the dike or rather wave reflection at the dike cannot be excluded. The wave reflection analysis at position 4 cannot be performed with the method by Mansard and Funke (1980), because the geometrical criterion (distance to the structure) is not fulfilled, which is why there are no results shown for the reflection in front of the dike.

Wave Transmission and Reduction of Wave Height

A mean wave height reduction of 23% or transmission coefficient $K_{t(4,2)}=0.77$ ($n=28$; with standard deviation of 0.124) has been found in the reference case (without vegetation) due to wave transformation on the foreshore. By including foreshore vegetation, the mean transmission coefficient results to $K_{t(4,2)}=0.68$ ($n=191$; with a standard deviation of 0.144), which converts to

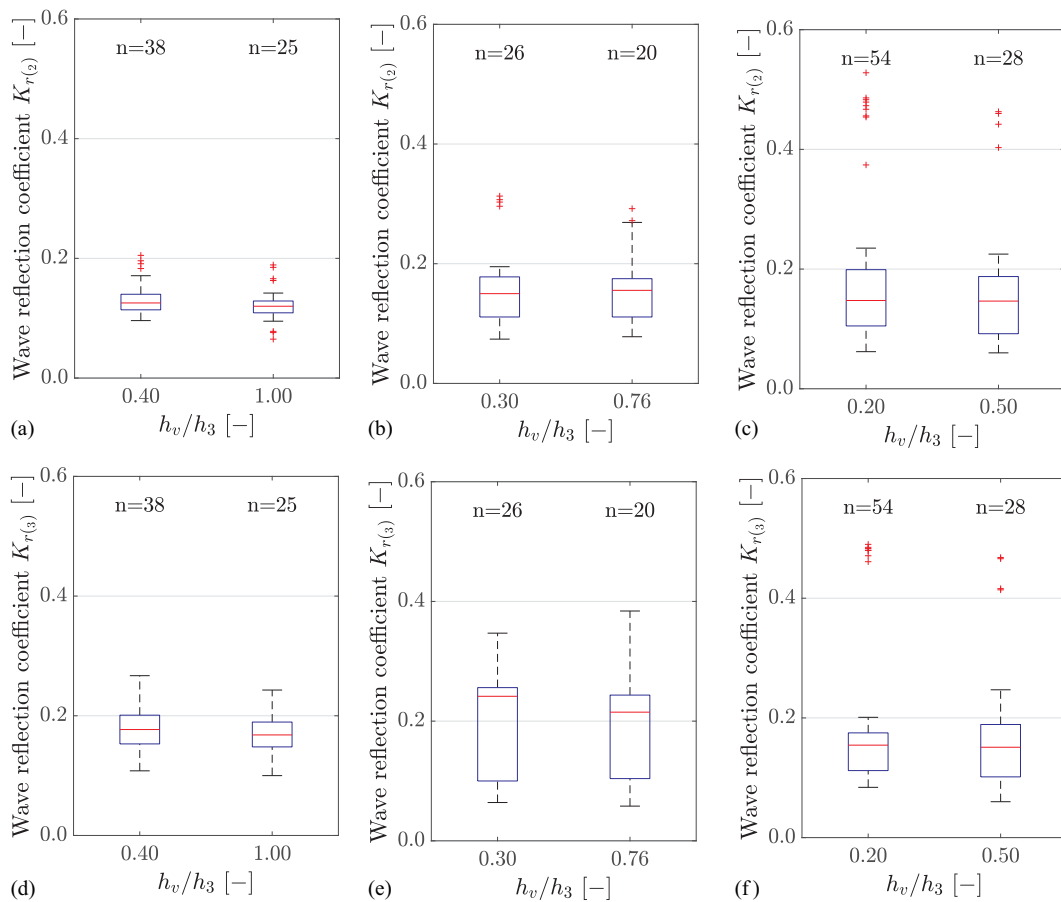


Fig. 5. Effect of the relative vegetation height h_v/h_3 on the wave reflection coefficient in front of the foreshore (position 2) and in front of the vegetation (position 3) with number of data points n and outliers (+) marked: (a) water depth $h_3 = 0.25$ m (position 2); (b) water depth $h_3 = 0.33$ m (position 2); (c) water depth $h_3 = 0.50$ m (position 2); (d) water depth $h_3 = 0.25$ m (position 3); (e) water depth $h_3 = 0.33$ m (position 3); and (f) water depth $h_3 = 0.50$ m (position 3).

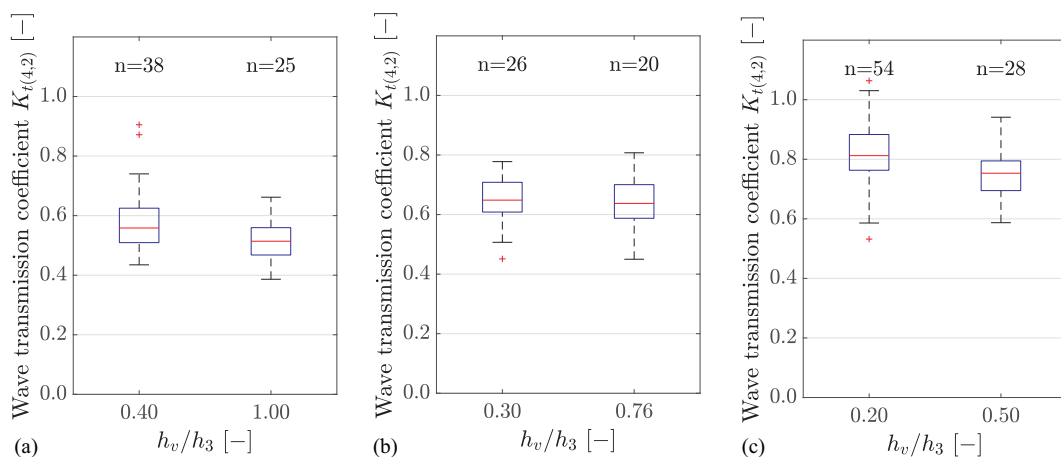


Fig. 6. Effect of the relative vegetation height h_v/h_3 on the wave transmission coefficient $K_{t(4,2)}$ with number of data points n and outliers (+) marked: (a) water depth $h_3 = 0.25$ m; (b) water depth $h_3 = 0.33$ m; and (c) water depth $h_3 = 0.50$ m.

a mean wave height reduction of 32% caused by the shallow foreshore and surrogate vegetation. In essence, mean wave height reductions of about 9% remain, where effects of the vegetation are considered only.

As wave transmission is equally dependent on water depth above the elevated foreshore, Fig. 6 depicts the wave transmission

coefficient $K_{t(4,2)} = H_{m0,4}/H_{m0,2}$ for the investigations with foreshore vegetation in correlation to the relative vegetation height h_v/h_3 for the water depths $h_3 = 0.25$, $h_3 = 0.33$, and $h_3 = 0.50$ m. The results for all meadow configurations are shown in Fig. 6 to examine the range of wave transmission as a function of varying incoming wave parameters.

The wave transmission for the vegetated tests ranges from median values of $K_{t(4,2)} = 0.81$ in case of $h_v = 0.10$ m ($h_v/h_3 = 0.20$) down to $K_{t(4,2)} = 0.51$ in case of $h_v = 0.25$ m ($h_v/h_3 = 1.00$). Fig. 6 shows a high influence of the water depth on wave transmission. For each water depth, the transmission is higher with the smaller vegetation height $h_v = 0.10$ m, but since the meadow displays relative low densities, the difference of the median wave attenuation values is low with 0.04 for $h_3 = 0.25$ m, 0.01 for $h_3 = 0.33$ m, and 0.06 for $h_3 = 0.50$ m. The transmission coefficients $K_{t(4,2)}$ for each vegetation configuration are summarized in Table 5 depending on the meadow width (B_v), the meadow height (h_v) and the meadow density (n_v). In addition to the dependence on water depth (as seen in Fig. 6), separating the results for different meadow configurations shows wave transmission as a function of vegetation density and meadow width. By comparing configurations 1 and 2 for $h_v = 0.25$ m with different vegetation densities, a higher transmission for a lower density can be identified. This effect is not apparent for configurations 3 and 4 with the lower vegetation height $h_v = 0.10$ m. The highest transmission in regards to the meadow width was observed for $B_v = 7.5$ m. In addition, the transmission is lower for the larger vegetation height (configurations 1 and 4 for 400 m^{-2} and configurations 2 and 3 for 200 m^{-2} vegetation height).

Reduction of Wave Set-up

The effect of the relative vegetation height h_v/h_3 on the reduction of the wave set-up η_s is shown in Fig. 7 for each water depth with $h_v = 0.10$ m in the left boxplot in each subfigure and $h_v = 0.25$ m in the right boxplot in each subfigure. The results for all

Table 5. Transmission coefficients $K_{t(4,2)}$ of different surrogate meadows

Configuration (-)	Surrogate meadow			Transmission coefficient $K_{t(4,2)}$ (-)
	B_v (m)	h_v (m)	n_v (m^{-2})	
0 (reference)	0.0	0.00	0	0.771 ± 0.124
1	5.0	0.25	400	0.613 ± 0.126
2	5.0	0.25	200	0.660 ± 0.126
3	5.0	0.10	200	0.707 ± 0.148
4	5.0	0.10	400	0.720 ± 0.144
5	7.5	0.10	400	0.664 ± 0.130
6	2.5	0.10	400	0.715 ± 0.171

meadow configurations are shown in this figure, which results in the incoming wave parameters as the reason for the range of wave set-up. The tests with surrogate meadows were compared with the reference tests twice (see the section “Experimental Program”). Therefore, each hydraulic condition is compared up to four times which provides a higher accuracy and an improved detection of outliers. This leads to a higher number of data points for the wave set-up and the wave run-up compared with the reflection and transmission.

In the presence of vegetation, the wave set-up η_s was reduced by up to 17.0% in case of $h_v/h_3 = 1.00$. This observation leads to the conclusion that the wave set-up is not increased by an obstructed return flow seawards, as was hypothesized earlier, at least given the modeled vegetation densities considered in this study. Instead, the wave set-up decreased in the presence of foreshore vegetation, as a result of its wave attenuating character. In addition, these results reveal a higher reduction of wave set-up for an increasing vegetation height indicated by the difference by each two datasets. In case of $h_3 = 0.25$ m the reduction of the wave set-up is 12.1% higher for the larger vegetation height. With increasing water depth, the effect of wave set-up reduction is also reduced. For $h_3 = 0.33$ m the difference between the median values for both vegetation heights is 6.0% and with $h_3 = 0.50$ m the reduction with $h_v = 0.25$ m is 3.1% higher than with $h_v = 0.10$ m. It should be noted that this observation is valid for 81% of the data points, whereas the reduction of the wave set-up is negative or rather below zero for 19% of the data points, which indicates a higher wave set-up than for the reference case. The mean value of the negative wave set-up however is only at -2.05% . This might depend on superposition of the incident and reflected waves in front of the dike for specific conditions and locations. A connection was not found in this case. This needs to be investigated in future studies.

Table 6 lists the mean reduction of the wave set-up and the standard deviation for each meadow configuration depending on the meadow width (B_v), the meadow height (h_v) and the meadow density (n_v). Comparing different vegetation densities (configurations 1 and 2 for $h_v = 0.25$ m; configurations 3 and 4 for $h_v = 0.10$ m), a higher mean wave set-up reduction can be correlated to a higher density, which supports the conclusion that the wave set-up is reduced due to the wave height reduction. Comparing different vegetation heights (configurations 1 and 4 for 400 m^{-2} ; configurations 2 and 3 for 200 m^{-2}), a higher wave set-up reduction is apparent with a increasing vegetation height. For the varying meadow widths, the highest wave set-up reduction appears for $B_v = 7.5$ m.

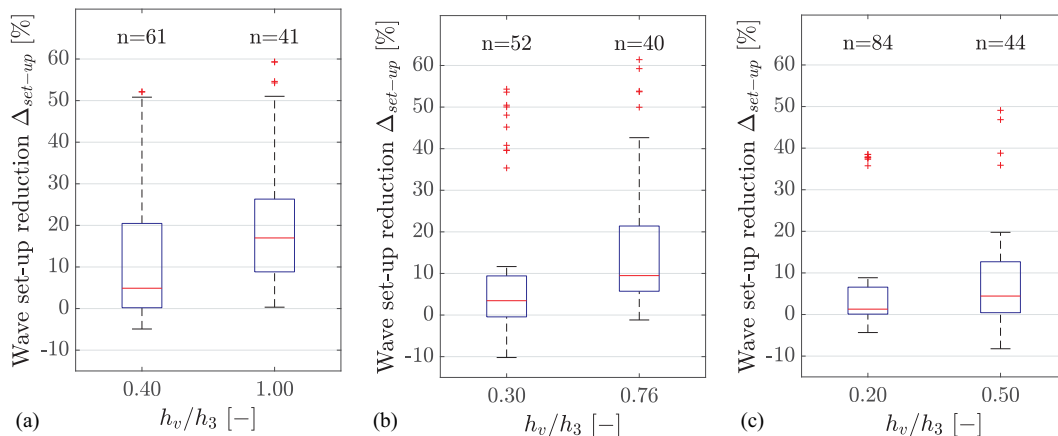


Fig. 7. Effect of the relative vegetation height h_v/h_3 on the wave set-up η_s with number of data points n and outliers (+) marked: (a) water depth $h_3 = 0.25$ m; (b) water depth $h_3 = 0.33$ m; and (c) water depth $h_3 = 0.50$ m.

Reduction of Wave Run-up

Finally, another objective in this work was the interaction of wave, vegetation and dike, with a focus on the wave run-up on the sloped dike ($\tan \alpha = 1 : 6$), the main parameter for the design of coastal defense structures. The mean wave run-up reduction due to foreshore vegetation is 9.6%. Fig. 8 shows the effect of the relative vegetation height h_v/h_3 on the reduction of the wave run-up height $R_{u2\%}$ for the different water depths. The left boxplot in each subfigure shows the results for the vegetation height $h_v = 0.10$ m and each right boxplot shows $h_v = 0.25$ m. Fig. 8 shows the range of wave run-up depending on varying incoming wave parameters since the results for all meadow configurations are shown.

The median values of the reduction of the wave run-up height $R_{u2\%}$ varies from about 2.3% at high water levels ($h_v/h_3 = 0.20$) up to 16.5% ($h_v/h_3 = 1.00$). Although a significant increase of 11.9% in wave run-up reduction with higher vegetation height at a low water depth $h_3 = 0.25$ m is apparent, it is decreasing with increasing water depth. For $h_3 = 0.33$ m the difference in run-up reduction is 7.6% and for the highest water depth $h_3 = 0.50$ m, the difference in wave run-up reduction with 2.7% at a high submergence is negligible. This actually shows the increasing wave attenuation with larger vegetation heights, but also the decreasing influence of vegetation on wave-related foreshore processes with higher submergence including some scattering due to model and potential scale effects.

However, 10% of the data points for the reduction of the wave run-up show a negative value which states a higher wave run-up for a vegetated foreshore compared with the reference case as seen previously for the wave set-up. The mean value of the negative results equates to -2.62% . The mean reduction of the wave run-up and the standard deviation for

each vegetation configuration are summarized in Table 7 depending on the meadow width (B_v), the meadow height (h_v), and the meadow density (n_v).

Comparing the reduction of wave run-up for different meadows shows differences, depending on vegetation densities, heights, and meadow widths. The results of this study show a higher wave run-up reduction with higher meadow density for $h_v = 0.25$ m (configurations 1 and 2), whereas no significant change in wave run-up is apparent for $h_v = 0.10$ m (configurations 3 and 4) in correlation to the density. In contrast, a higher wave run-up reduction can be seen for both cases of increasing vegetation heights (configurations 1 and 4 for 400 m^{-2} ; configurations 2 and 3 for 200 m^{-2}). The influence of the meadow width can be seen slightly, although it is not significant (configurations 4, 5, and 6). Further investigations are, however, needed to quantify the effect of the meadow, and to reliably link additional vegetation parameters with statistical confidence. In addition, the comparison of the wave run-up generating a JONSWAP-spectrum or regular waves shows a mean difference of $0.48\% (\pm 1.10\%; n = 8)$, which is why regular waves were used to investigate the influence of surrogate vegetation in this study. However, additional investigations are necessary to quantify the difference by generating regular waves in the case of foreshore geometry and vegetation.

Discussion

Looking at the results of this study, a mean wave height reduction of only 9% due to foreshore vegetation was observed. However, it has to be noted that relatively low densities (Abu Hena et al. 2007; van Veelen et al. 2020) and marsh widths as well as high submergence

Table 6. Reduction of wave set-up η_s of different surrogate meadows

Configuration (-)	Surrogate meadow			Reduction of wave set-up η_s (%)
	B_v (m)	h_v (m)	n_v (m^{-2})	
1	5.0	0.25	400	19.4 ± 17.0
2	5.0	0.25	200	12.1 ± 15.8
3	5.0	0.10	200	7.4 ± 15.4
4	5.0	0.10	400	8.3 ± 14.6
5	7.5	0.10	400	11.5 ± 16.0
6	2.5	0.10	400	8.4 ± 14.6

Table 7. Reduction of wave run-up $R_{u2\%}$ of different surrogate meadows

Configuration (-)	Surrogate meadow			Reduction of wave run-up $R_{u2\%}$ (%)
	B_v (m)	h_v (m)	n_v (m^{-2})	
1	5.0	0.25	400	15.7 ± 14.4
2	5.0	0.25	200	10.4 ± 11.5
3	5.0	0.10	200	6.7 ± 11.0
4	5.0	0.10	400	6.9 ± 9.9
5	7.5	0.10	400	9.6 ± 12.1
6	2.5	0.10	400	6.6 ± 9.8

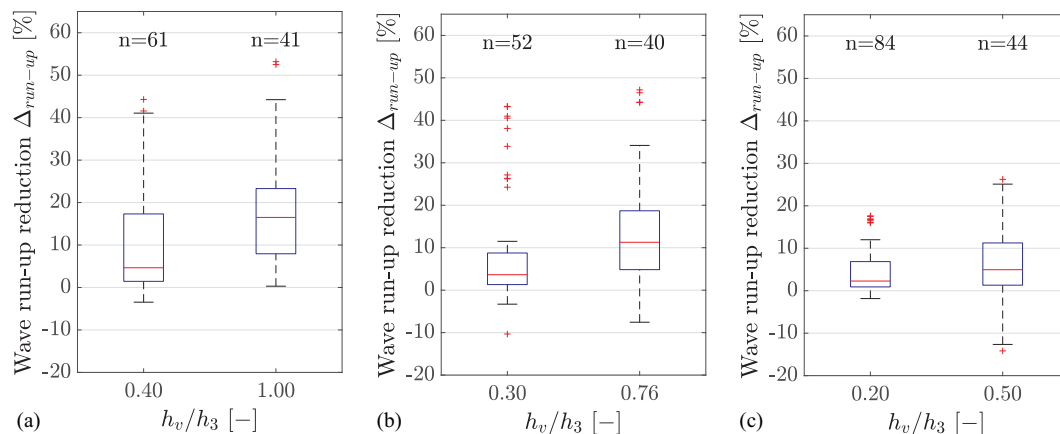


Fig. 8. Effect of the relative vegetation height h_v/h_3 on the reduction of the wave run-up $R_{u2\%}$ with number of data points n and outliers (+) marked: (a) water depth $h_3 = 0.25$ m; (b) water depth $h_3 = 0.33$ m; and (c) water depth $h_3 = 0.50$ m.

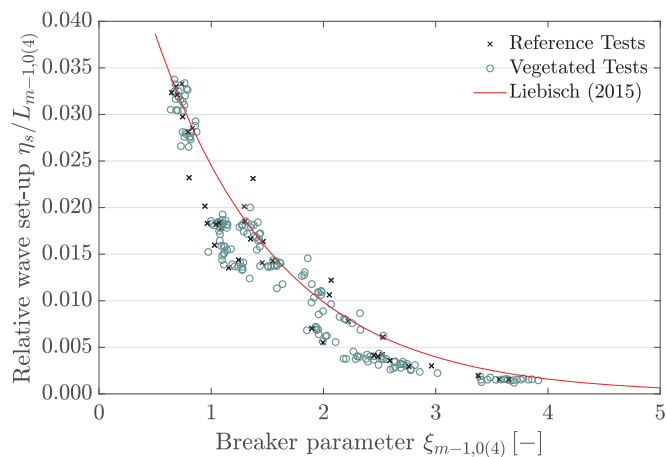


Fig. 9. Effect of surf similarity parameter $\xi_{m-1,0(4)}$ on the relative wave set-up $\eta_s/L_{m-1,0(4)}$.

ratios were investigated. Furthermore, the importance of foreshore vegetation in coastal engineering is not solely a matter of roughness effects and wave energy dissipation. Root systems stabilize the foreshore and reduce erosion (Ford et al. 2016) or even enable growth of the foreshore (Cahoon et al. 1996). This results in high wave energy reduction due to foreshore geometry (as seen in this study), which might be damaged in storm surges and lead to less-effective impeding wave energy reduction and therefore coastal protection. To fully understand the benefits of foreshore vegetation in coastal protection, more comprehensive study designs joining biomechanic, ecohydraulic, and morphodynamic processes need to be developed.

To compare the results of this study to existing equations derived in preceding investigations, the results for the surf similarity parameter $\xi_{m-1,0}$ are shown as a function of the relative wave set-up $\eta_s/L_{m-1,0}$ in Fig. 9 as presented in Liebisch (2015). The surf similarity parameter $\xi_{m-1,0}$ for this study is determined based on the wave length $L_{m-1,0}$ with the spectral wave period $T_{m-1,0}$. The tests of Liebisch (2015) omitted a shallow foreshore profile in the experiments; instead a smooth, sloped dike profile similar to this work, with a slope of $\cot \alpha = 6$ was solely used. Consequently, any comparison of the results in this study with results presented by Liebisch (2015) requires caution. The focus for this comparison here is put on the wave set-up at the dike profile, because neither a foreshore nor vegetation are part of the investigations. For the calculation of $\eta_s/L_{m-1,0}$ and $\xi_{m-1,0}$ the wave properties measured in front of the dike (H_{m0} , $T_{m-1,0}$) were used to determine a theoretical deep-water wave length.

The results of this study show significant comparability to the equation presented by Liebisch (2015) for a 1:6 dike slope. The difference in relative wave set-up between the reference tests and the tests including a surrogate meadow as a function of the surf similarity parameter is not recognizable. Further investigations need to determine the applicability of Eq. (6) considering vegetated foreshores.

In addition, the results of this study are compared with the equation for wave run-up from EurOtop (2018). Fig. 10 shows both datasets using the wave parameters in front of the dike (position 4) as proposed by EurOtop (2018) with a solid line as regression for the reference tests and a dashed line for the configurations investigating a vegetated foreshore.

Comparing the relative wave run-up $R_{u2\%}/H_{m0(4)}$ for the reference tests to the tests including a surrogate meadow, only a moderate difference can be seen. There are apparent differences between the (EurOtop 2018) equations and the results of this investigation;

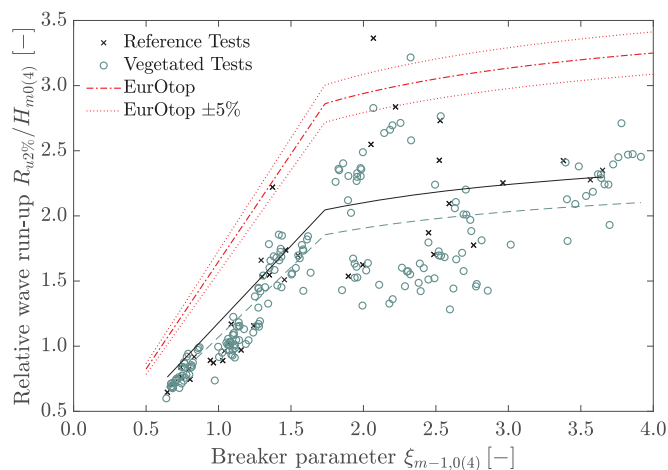


Fig. 10. Comparing laboratory results with EurOtop (2018) equations for wave run-up.

Table 8. Adaptation of the EurOtop (2018) equations to include the effects of vegetated foreshores

Position in Flume	Experiments	Adapting Eq. (8)			Adapting Eq. (9)		
		Factor	R^2	n	Factor	R^2	n
	EurOtop (2018)	1.65	—	—	1.00	—	—
Position 2	Reference Tests	1.23	0.59	48	0.75	0.14	16
	Vegetated Tests	1.16	0.57	147	0.70	0.21	44
Position 4 (see Fig. 10)	Reference Tests	1.18	0.68	36	0.72	-0.03	28
	Vegetated Tests	1.07	0.85	104	0.65	0.02	87

foremost, these seem to originate from the fact that the (EurOtop 2018) equations are not meant to be used where a considerable foreshore geometry is present. Hence, the influence of the foreshore geometry on the relative wave run-up is not predominant in Fig. 10, whereas the effect of the vegetation is only moderate. The equations given in EurOtop (2018) are not readily applicable for a dike profile with a foreshore. In Table 8 the adapted factors for the equations are given along with the coefficient of determination R^2 and the number of data points n used to determine the adaptation. An assumed condition is the intersection of the two regressions at $\xi_{m-1,0} = 1.74$ after EurOtop (2018) and to only adjust the factors for the two equations, which renders those interdependent. Accordingly, the best fit of factors was selected.

For a comprehensive comparison, Table 8 shows the adapted factors using both, incoming wave properties at position 2 as well as position 4. The results for position 2 therefore include the influence of the foreshore, whereas position 4 uses the incoming wave properties as seen in EurOtop (2018).

By looking at the results of this study for the wave set-up and the wave run-up relatively (relative wave set-up $\eta_s/L_{m-1,0}$ and relative wave run-up $R_{u2\%}/H_{m0}$), the increased values compared with reference tests for the reduction of the wave set-up and the wave run-up were not apparent as seen in the results. To understand the difference in wave set-up and wave run-up as a function of meadow properties, these need to be more significant. Higher ranges of vegetation densities as well as widths (considering scaling) need to be investigated to elucidate a potential influence of the vegetation more clearly and to model salt marshes more realistically.

The focus of this study were the hydraulics on the vegetated foreshore and the data has been analyzed regarding the relevant processes. The results of this study contain additional information, such as wave run-down, change in wave spectra (frequency shift), transmission within the artificial vegetation, and bending behavior through under water cameras. Upon request these results are available for future investigations considering hydraulic processes in vegetated foreshores.

Conclusions

Several investigations have been carried out to examine the ecohydraulic effect of vegetation with surrogate salt marsh vegetation (Anderson and Smith 2014; Augustin et al. 2009; Koftis et al. 2013; Mei et al. 2011). Analyzing wave transmission presents a wave absorption once waves have propagated across the foreshore setup. To date, however, very little research has investigated the combined effect of realistic coastal shoreline profiles in combination with vegetation on the shore; as wave–vegetation and shallow-water wave transformations typically coevolve, this work, for the first time to the best of the authors' knowledge, analyses and discusses these effects scientifically. The laboratory experiments carried out in this study explore the wave transmission as well as the effects on wave set-up and run-up in front of a dike profile for a wide spectrum of wave properties. The effects were analyzed and compared for different meadow configurations and reference tests. For long wave periods, considerable dispersion of the generated waves was observed because intermediate and shallow-water conditions were apparent; this can be explained by roughness effects and significant wave–wave interaction across the foreshore profile. Owing to the wave transformation between the wave maker and the setup, the incoming wave properties in front of the setup were used to analyze the processes on the foreshore and at the dike.

Looking at the wave reflection at the toe of the foreshore geometry, the influence of the vegetation is not apparent, but median values between 0.120 ($h_v/h_3 = 1.00$) and 0.156 ($h_v/h_3 = 0.76$) were observed depending on foreshore geometry and water depth. In front of the surrogate meadow the wave reflection shows small differences for a varying vegetation height and increasing reflection with decreasing water depth. All in all, median values between 0.151 ($h_v/h_3 = 0.50$) and 0.242 ($h_v/h_3 = 0.30$) are present in this study. The reflection in front of the vegetation meadow is higher than in front of the foreshore.

Examining the wave transmission, a mean value of 0.77 is present in the reference cases without vegetation contrasted by 0.68 mean transmission with vegetation. This results in a mean wave height reduction of 9% due to vegetation. Comparing different vegetation heights shows decreasing wave transmission or rather increasing wave height reduction for larger vegetation, with differences in median values between 0.01 and 0.06 depending on water depth (increasing transmission with increasing water depth). In addition, a higher transmission for lower vegetation densities can be seen in the results as well as a higher transmission with decreasing meadow width.

It could be shown that integrating foreshore vegetation into current sea dike designs, reduces the wave set-up and the wave run-up. For the wave set-up reduction, median values up to 17.0% were observed because the local wave heights are reduced due to wave attenuation through the meadow. The reduction of the wave set-up increased with a higher vegetation density, height, and meadow width. Future investigations should examine whether reduced return flow occurs as a consequence for significantly higher

vegetation densities. A wave run-up reduction up to 16.5% was observed with decreasing water depths and increasing vegetation heights (increasing relative vegetation heights) in this study.

This systematic study shows the interaction between wave, vegetation, and sea dike as well as different wave transformation processes with each other for a low meadow density and different submergence ratios as well as meadow widths. The load-reducing potential of foreshore vegetation is elucidated by examining the wave transmission, wave set-up, and wave run-up. It is noted that these processes also interact. Naturally, showing results of individual processes includes the influence of other processes. Results identify the submergence ratio as an important parameter. Other parameters did not show an explicit trend, and remain difficult to be evaluated when investigating hydrodynamic processes on vegetated foreshores.

The mechanical properties of the vegetation model, such as elastic forces and the dynamic behavior under wave action were not designed for a specific plant species because the primary goal of these tests was to arrive at a better understanding of wave transformation processes and to determine important parameters. To fully understand and quantify the ecohydraulic effects of foreshore vegetation and the interactions of flow and vegetation, a vegetation model considering the relevant parameters needs to be developed in future research; for example, biomass above and below ground (Feagin et al. 2019; Schoutens et al. 2020; Schulze et al. 2019), shoot density (Möller 2006; Rupprecht et al. 2015), and Young's bending modulus or even flexural rigidity (Rupprecht et al. 2015; Schoutens et al. 2020; Schulze et al. 2019; Vuik et al. 2018; Zhu et al. 2019; Liu et al. 2021) constitute elemental research questions to be investigated and answered in followup studies.

The arrangement of the individual plant specimen that constituted the vegetation model were located on the foreshore in a regular pattern, and without typical plant elements such as leaves. Recent works have started to model coastal vegetation through numerical models; for example, by Hadadpour et al. (2019). There, the vegetation was approximated by a porous media and correlated with the area leaf index to match vegetation properties. Lightbody and Nepf (2006) also highlight the need to use the frontal area of plants when assessing their effects on and interaction with environmental flows. To better understand vegetation effects on the attenuation of waves, further investigations should be conducted to also understand the combined effects of plant stems and leaves, an effect beyond the scope of this work.

Future investigation regarding the ecohydraulic effects of foreshore vegetation should consider the following issues.

- Modeling of biomechanical vegetation properties such as geometry, elastic forces, rigidity, and dynamic behavior as well as scaling these properties. This study shows a systematic approach because field studies need to be carried out for the development of a scaled vegetation model.
- Investigating the interaction between wave, current, and vegetation, because current studies mostly determine only the effect of wave–vegetation interaction.
- To avoid scale and model effects, large-scale models need to be carried out in order to quantify the effects and processes.
- Large range of different arrangements regarding bed width, density, height, and submergence ratio. In this study, varying densities and meadow widths were investigated but the range of influence was smaller than the influence of varying wave properties. This leads to the conclusion that the characteristics in individual meadows need to be more profound than presented in this study.
- Combined vegetation structure of stems and leaves, because previous research predominantly focuses on vegetation stems.

- The inhomogeneity of coastal salt marshes needs to be modeled as well to determine the effects of different vegetation heights, densities, and rigidities in combination, which leads to the investigation of more realistic conditions. These need to be examined in order to refine current sea dike design guidelines and practices to develop a sustainable and ecologically friendly sea dike design incorporating the foreshore.

Data Availability Statement

Some or all data, models, or code that support the findings of this study are available from the corresponding author upon reasonable request (i.e., data on wave reflection, transmission, set-up, and run-up).

Acknowledgments

The authors acknowledge the financial support by the Federal Ministry of Education and Research (BMBF) in the framework of the EcoDike project SP3.3 (Grant ID No. 03F0757B).

References

- Abu Hena, M., F. Short, S. Sharifuzzaman, M. Hasan, M. Rezowan, and M. Ali. 2007. "Salt marsh and seagrass communities of Bakkhali estuary, Cox's Bazar, Bangladesh." *Estuarine Coastal Shelf Sci.* 75 (1–2): 72–78. <https://doi.org/10.1016/j.ecss.2007.01.022>.
- Altomare, C., T. Suzuki, X. Chen, T. Verwaest, and A. Kortenhuis. 2016. "Wave overtopping of sea dikes with very shallow foreshores." *Coastal Eng.* 116: 236–257. 1
- Anderson, M. E., and J. M. Smith. 2014. "Wave attenuation by flexible, idealized salt marsh vegetation." *Coastal Eng.* 83: 82–92. <https://doi.org/10.1016/j.coastaleng.2013.10.004>.
- Anderson, M. E., J. M. Smith, D. B. Bryant, and R. G. McComas. 2013. *Laboratory studies of wave attenuation through artificial and real vegetation*. Report Number ERDC TR-13-11. Engineer Research and Development Center.
- Ardani, S., and J. M. Kaihatu. 2019. "Evolution of high frequency waves in shoaling and breaking wave spectra." *Phys. Fluids* 31 (8): 087102. <https://doi.org/10.1063/1.5096179>.
- Augustin, L. N., J. L. Irish, and P. Lynett. 2009. "Laboratory and numerical studies of wave damping by emergent and near-emergent wetland vegetation." *Coastal Eng.* 56 (3): 332–340. <https://doi.org/10.1016/j.coastaleng.2008.09.004>.
- Barbier, E. B., S. D. Hacker, C. Kennedy, E. W. Koch, A. C. Stier, and B. R. Silliman. 2011. "The value of estuarine and coastal ecosystem services." *Ecol. Monogr.* 81 (2): 169–193. <https://doi.org/10.1890/10-1510.1>.
- Bouma, T. J., M. B. de Vries, and P. M. J. Herman. 2010. "Comparing ecosystem engineering efficiency of two plant species with contrasting growth strategies." *Ecology* 91 (9): 2696–2704. <https://doi.org/10.1890/09-0690.1>.
- Cahoon, D. R., J. C. Lynch, and A. N. Powell. 1996. "Marsh vertical accretion in a Southern California Estuary, USA." *Estuarine Coastal Shelf Sci.* 43 (1): 19–32. <https://doi.org/10.1006/ecss.1996.0055>.
- Carus, J., M. Paul, and B. Schröder. 2016. "Vegetation as self-adaptive coastal protection." *Ecol. Evol.* 6 (6): 1579–1589. <https://doi.org/10.1002/ece3.2016.6.issue-6>.
- CERC. 1984. "Shore protection manual: Volume I." *SPM 1984*. U.S. Army Engineer Waterways Experiment Station Coastal Engineering Research Center (CERC).
- Christie, E., I. Möller, M. Schuerch, B. Evans, and H. Brooks. 2019. "Modelling sensitivity to erosion by waves and tides on an open coast salt-marsh." In Vol. 21 of *21st EGU General Assembly, Proc. from the Conf.* Geophysical Research Abstracts. Accessed July 16, 2020. <https://meetingorganizer.copernicus.org/EGU2019/EGU2019-15914.pdf>.
- Dean, R. G., and C. J. Bender. 2006. "Static wave set-up with emphasis on damping effects by vegetation and bottom friction." *Coastal Eng.* 53 (2–3): 149–156. <https://doi.org/10.1016/j.coastaleng.2005.10.005>.
- Dean, R. G., and T. L. Walton. 2010. "Wave set-up." In *Handbook of coastal and ocean engineering*, edited by Y. C. Kim. Singapore: World Scientific.
- EuroTop. 2018. "Eurotop - manual on wave overtopping of sea defences and related structures." www.overtopping-manual.com.
- Feagin, R. A., M. Furman, K. Salgado, M. L. Martinez, R. A. Innocenti, K. Eubanks, J. Figlus, T. P. Huff, J. Sigren, and R. Silva. 2019. "The role of beach and sand dune vegetation in mediating wave run up erosion." *Estuarine Coastal Shelf Sci.* 219: 97–106. <https://doi.org/10.1016/j.ecss.2019.01.018>.
- Ford, H., A. Garbutt, C. Ladd, J. Malarkey, and M. W. Skov. 2016. "Soil stabilization linked to plant diversity and environmental context in coastal wetlands." *J. Veg. Sci.* 27 (2): 259–268. <https://doi.org/10.1111/jvs.2016.27.issue-2>.
- Goda, Y., and Y. Suzuki. 1977. "Estimation of incident and reflected waves in random wave experiments." In *Proc., 15th Coastal Engineering Conf.*, 828–845. Reston, VA: ASCE.
- Hadadpour, S., M. Paul, and H. Oumeraci. 2019. "Numerical investigation of wave attenuation by rigid vegetation based on a porous media approach." *J. Coastal Res.* 2019 (92): 92–100. <https://doi.org/10.2112/SI92-011.1>.
- Hanley, M. E., et al. 2014. "Shifting sands? Coastal protection by sand banks, beaches and dunes." *Coastal Eng.* 87: 136–146. <https://doi.org/10.1016/j.coastaleng.2013.10.020>.
- Hu, Z., T. Suzuki, T. Zitman, W. Uittewaal, and M. Stive. 2014. "Laboratory study on wave dissipation by vegetation in combined current-wave flow." *Coastal Eng.* 88: 131–142. <https://doi.org/10.1016/j.coastaleng.2014.02.009>.
- Hughes, S. A. 1993. "Laboratory wave reflection analysis using co-located gages." *Coastal Eng.* 20 (3–4): 223–247. [https://doi.org/10.1016/0378-3839\(93\)90003-Q](https://doi.org/10.1016/0378-3839(93)90003-Q).
- John, B. M., K. G. Shirlal, and S. Rao. 2015. "Effect of artificial sea grass on wave attenuation - an experimental investigation." *Aquat. Procedia* 4: 221–226. <https://doi.org/10.1016/j.aqpro.2015.02.030>.
- Kathiresan, K., and N. Rajendran. 2005. "Coastal mangrove forests mitigated tsunami." *Estuarine Coastal Shelf Sci.* 65 (3): 601–606. <https://doi.org/10.1016/j.ecss.2005.06.022>.
- King, S. E., and J. N. Lester. 1995. "The value of salt marsh as a sea defence." *Mar. Pollut. Bull.* 30 (3): 180–189. [https://doi.org/10.1016/0025-326X\(94\)00173-7](https://doi.org/10.1016/0025-326X(94)00173-7).
- Koch, E. W., et al. 2009. "Non-linearity in ecosystem services: Temporal and spatial variability in coastal protection." *Front. Ecol. Environ.* 7 (1): 29–37. <https://doi.org/10.1890/080126>.
- Koftis, T., P. Prinos, and V. Stratigaki. 2013. "Wave damping over artificial *Posidonia oceanica* meadow: A large-scale experimental study." *Coastal Eng.* 73: 71–83. <https://doi.org/10.1016/j.coastaleng.2012.10.007>.
- Leonardi, N., I. Carnacina, C. Donatelli, N. K. Ganju, A. J. Plater, M. Schuerch, and S. Temmerman. 2018. "Dynamic interactions between coastal storms and salt marshes: A review." *Geomorphology* 301: 92–107. <https://doi.org/10.1016/j.geomorph.2017.11.001>.
- Leonardi, N., and S. Fagherazzi. 2015. "Effect of local variability in erosional resistance on large-scale morphodynamic response of salt marshes to wind waves and extreme events." *Geophys. Res. Lett.* 42 (14): 5872–5879. <https://doi.org/10.1002/2015GL064730>.
- Liebisch, S. 2015. "Bonded porous revetments – effect of porosity on wave-induced loads and hydraulic performance – An experimental study –." Technische Universität Braunschweig.
- Lightbody, A. F., and H. M. Nepf. 2006. "Prediction of velocity profiles and longitudinal dispersion in salt marsh vegetation." *Limnol. Oceanogr.* 51 (1): 218–228. <https://doi.org/10.4319/lo.2006.51.1.0218>.
- Liu, J., S. Kutschke, K. Keimer, V. Kosmalla, D. Schürenkamp, N. Goseberg, and M. Böhl. 2021. "Experimental characterisation and three-dimensional modelling of elymus for the assessment of ecosystem services." *Ecol. Eng.* 166: 106233. <https://doi.org/10.1016/j.ecoleng.2021.106233>.
- Maddock, I. P., A. Harby, P. Kemp, and P. J. Wood. 2013. *Ecohydraulics*. Hoboken, NJ: John Wiley & Sons.
- Mahmoudof, S. M., P. Badieli, S. M. Siadatmousavi, and V. Chegini. 2016. "Observing and estimating of intensive triad interaction occurrence in

- very shallow water." *Cont. Shelf Res.* 122: 68–76. <https://doi.org/10.1016/j.csr.2016.04.003>.
- Mansard, E. P. D., and E. R. Funke. 1980. "The measurement of incident and reflected spectra using a least squares method." *Coastal Eng.* 1 (17): 8. <https://doi.org/10.9753/icce.v17.8>.
- Maza, M., J. L. Lara, I. J. Losada, B. Ondiviela, J. Trinogga, and T. J. Bouma. 2015. "Large-scale 3-d experiments of wave and current interaction with real vegetation." *Coastal Eng.* 107: 70–83.
- McCowan, J. 1891. "On the solitary wave." *Lond. Edinb. Dubl. Phil. Mag. J. Sci.* 32 (194): 45–58. <https://doi.org/10.1080/14786449108621390>.
- Mei, C. C., I.-C. Chan, P. L.-F. Liu, Z. Huang, and W. Zhang. 2011. "Long waves through emergent coastal vegetation." *J. Fluid Mech.* 687: 461–491. <https://doi.org/10.1017/jfm.2011.373>.
- Meselhe, E., Y. Wang, E. White, H. Jung, M. M. Baustian, S. Hemmerling, M. Barra, and H. Bienn. 2020. "Knowledge-based predictive tools to assess effectiveness of natural and nature-based solutions for coastal restoration and protection planning." *J. Hydraul. Eng.* 146 (2): 05019007. [https://doi.org/10.1061/\(ASCE\)HY.1943-7900.0001659](https://doi.org/10.1061/(ASCE)HY.1943-7900.0001659).
- Möller, I. 2006. "Quantifying saltmarsh vegetation and its effect on wave height dissipation: Results from a UK east coast saltmarsh." *Estuarine Coastal Shelf Sci.* 69 (3–4): 337–351. <https://doi.org/10.1016/j.ecss.2006.05.003>.
- Möller, I., et al. 2014. "Wave attenuation over coastal salt marshes under storm surge conditions." *Nat. Geosci.* 7: 727–731. <https://doi.org/10.1038/ngeo2251>.
- Nestler, J. M., R. A. Goodwin, D. L. Smith, and J. J. Anderson. 2008. "A mathematical and conceptual framework for ecohydraulics." In *Hydroecology and ecohydrology*. Hoboken, NJ: John Wiley & Sons.
- Paul, M., T. J. Bouma, and C. L. Amos. 2012. "Wave attenuation by submerged vegetation: Combining the effect of organism traits and tidal current." *Mar. Ecol. Prog. Ser.* 444: 31–41. <https://doi.org/10.3354/meps09489>.
- Peruzzo, P., F. de Serio, A. Defina, and M. Mossa. 2018. "Wave height attenuation and flow resistance due to emergent or near-emergent vegetation." *Water* 10 (4): 402. <https://doi.org/10.3390/w10040402>.
- Purcell, A. D., P. N. Khanal, T. J. Straka, and D. B. Willis. 2020. *Valuing ecosystem services of coastal marshes and wetlands*. Clemson, SC: Land-Grant Press by Clemson Extension. <https://doi.org/10.34068/report4>.
- Rupprecht, F., I. Möller, B. Evans, T. Spencer, and K. Jensen. 2015. "Biophysical properties of salt marsh canopies - quantifying plant stem flexibility and above ground biomass." *Coastal Eng.* 100: 48–57. <https://doi.org/10.1016/j.coastaleng.2015.03.009>.
- Schoutens, K., M. Heuner, E. Fuchs, V. Minden, T. Schulte-Ostermann, J.-P. Belliard, T. J. Bouma, and S. Temmerman. 2020. "Nature-based shoreline protection by tidal marsh plants depends on trade-offs between avoidance and attenuation of hydrodynamic forces." *Estuarine Coastal Shelf Sci.* 236: 106645. <https://doi.org/10.1016/j.ecss.2020.106645>.
- Schulze, D., F. Rupprecht, S. Nolte, and K. Jensen. 2019. "Seasonal and spatial within-marsh differences of biophysical plant properties: Implications for wave attenuation capacity of salt marshes." *Aquat. Sci.* 81: 65. <https://doi.org/10.1007/s00027-019-0660-1>.
- Silva, R., M. L. Martínez, I. Odériz, E. Mendoza, and R. A. Feagin. 2016. "Response of vegetated dune-beach systems to storm conditions." *Coastal Eng.* 109: 53–62. <https://doi.org/10.1016/j.coastaleng.2015.12.007>.
- Spencer, T., et al. 2016. "Salt marsh surface survives true-to-scale simulated storm surges." *Earth Surf. Processes Landforms* 41 (4): 543–552. <https://doi.org/10.1002/esp.v41.4>.
- Stockdon, H. F., R. A. Holman, P. A. Howd, and A. H. Sallenger. 2006. "Empirical parameterization of set-up, swash, and run-up." *Coastal Eng.* 53 (7): 573–588. <https://doi.org/10.1016/j.coastaleng.2005.12.005>.
- Tempest, J. A., I. Möller, and T. Spencer. 2015. "A review of plant-flow interactions on salt marshes: The importance of vegetation structure and plant mechanical characteristics." *Water* 2 (6): 669–681.
- Tschirky, P., K. Hall, and D. Turcke. 2001. "Wave attenuation by emergent wetland vegetation." In *Coastal Engineering 2000*, edited by B. L. Edge. [https://doi.org/10.1061/40549\(276\)67](https://doi.org/10.1061/40549(276)67).
- van Gent, M. R. A. 2001. "Wave run-up on dikes with shallow foreshores." *J. Waterway, Port, Coastal, Ocean Eng.* 127 (5): 254–262. [https://doi.org/10.1061/\(ASCE\)0733-950X\(2001\)127:5\(254\)](https://doi.org/10.1061/(ASCE)0733-950X(2001)127:5(254)).
- van Veelen, T. J., T. P. Fairchild, D. E. Reeve, and H. Karunarathna. 2020. "Experimental study on vegetation flexibility as control parameter for wave damping and velocity structure." *Coastal Eng.* 157: 103648. <https://doi.org/10.1016/j.coastaleng.2020.103648>.
- Vuik, V., H. Y. S. Heo, Z. Zhu, B. W. Borsje, and S. N. Jonkman. 2018. "Stem breakage of salt marsh vegetation under wave forcing: A field and model study." *Estuarine Coastal Shelf Sci.* 200: 41–58. <https://doi.org/10.1016/j.ecss.2017.09.028>.
- Vuik, V., S. N. Jonkman, B. W. Borsje, and T. Suzuki. 2016. "Nature-based flood protection." *Coastal Eng.* 116: 42–56. <https://doi.org/10.1016/j.coastaleng.2016.06.001>.
- Wu, W.-C., and D. T. Cox. 2015. "Effects of wave steepness and relative water depth on wave attenuation by emergent vegetation." *Estuarine Coastal Shelf Sci.* 164: 443–450. <https://doi.org/10.1016/j.ecss.2015.08.009>.
- Zhu, Z., Z. Yang, and T. J. Bouma. 2019. "Biomechanical properties of marsh vegetation in space and time: Effects of salinity, inundation and seasonality." *Ann. Bot.* 125 (2): 277–290. <https://doi.org/10.1093/aob/mcz063>.